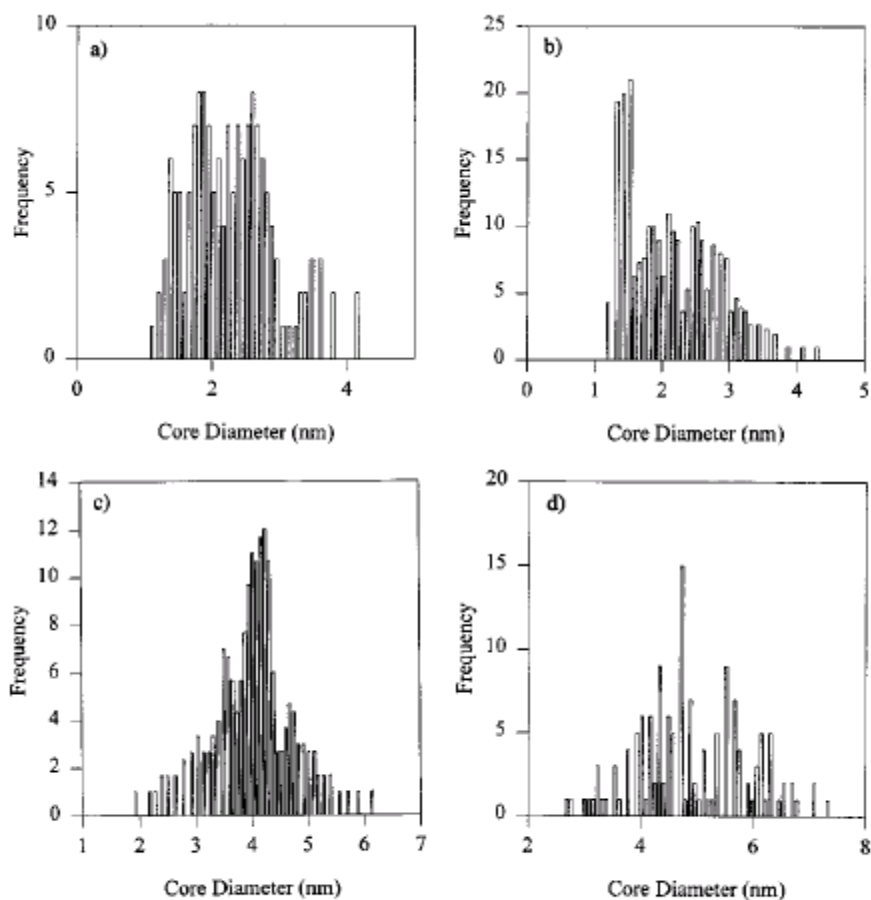
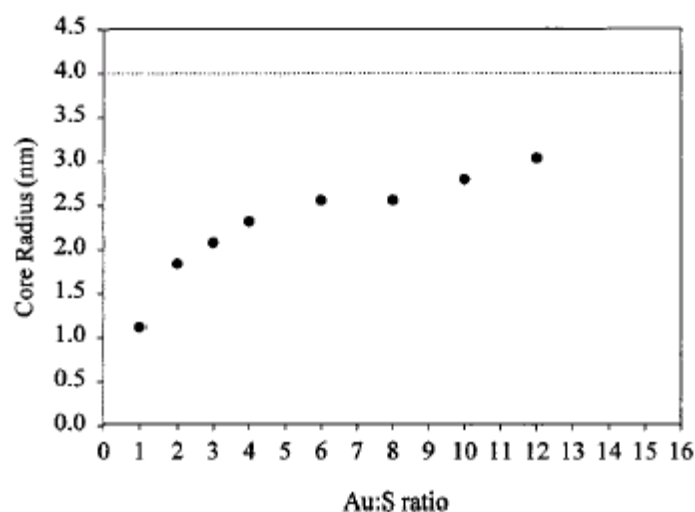


## Alkanethiolate Gold Cluster Molecules with Core Diameters from 1.5 to 5.2 nm: Core and Monolayer Properties as a Function of Core Size

Michael J. Hostetler,<sup>†</sup> Julia E. Wingate,<sup>†</sup> Chuan-Jian Zhong,<sup>‡</sup> Jay E. Harris,<sup>†</sup> Richard W. Vachet,<sup>†</sup> Michael R. Clark,<sup>†</sup> J. David Londono,<sup>§</sup> Stephen J. Green,<sup>†</sup> Jennifer J. Stokes,<sup>†</sup> George D. Wignall,<sup>§</sup> Gary L. Glish,<sup>†</sup> Marc D. Porter,<sup>‡</sup> Neal D. Evans,<sup>||</sup> and Royce W. Murray<sup>\*,†</sup>



**Figure 2.** Size histograms (a and d are for films shown in Figure 1): (a) (0°, 2X, fd); (b) (0°, 2X, sd); (c) (RT, 1/4X, fd); (d) (RT, 1/6X, fd).



**Figure 6.** Plot of the cluster core radius, calculated from  $^1\text{H}$  NMR line widths, as a function of Au:S ratio using during the cluster synthesis.

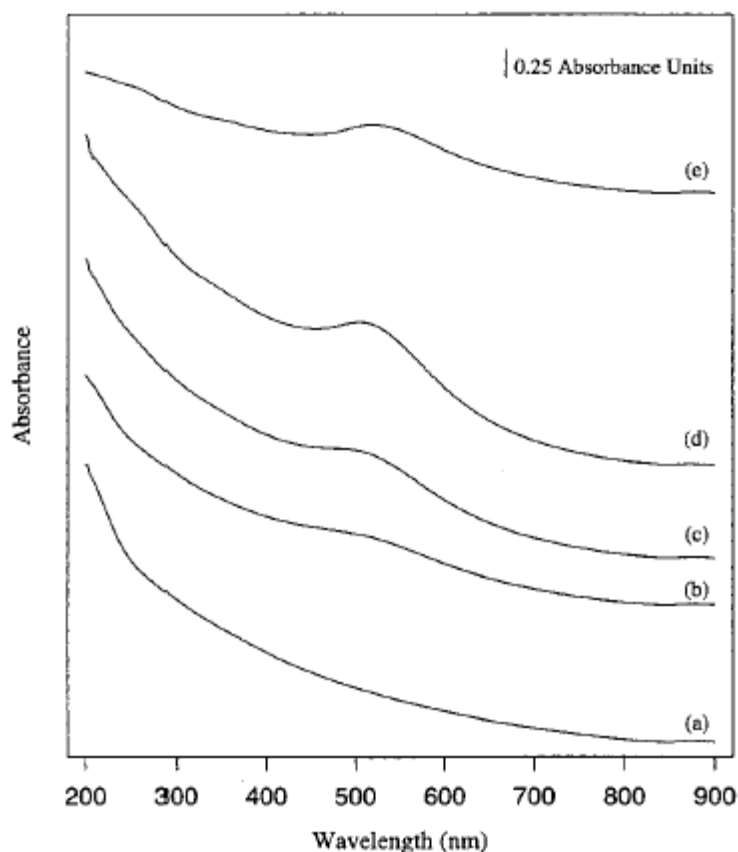
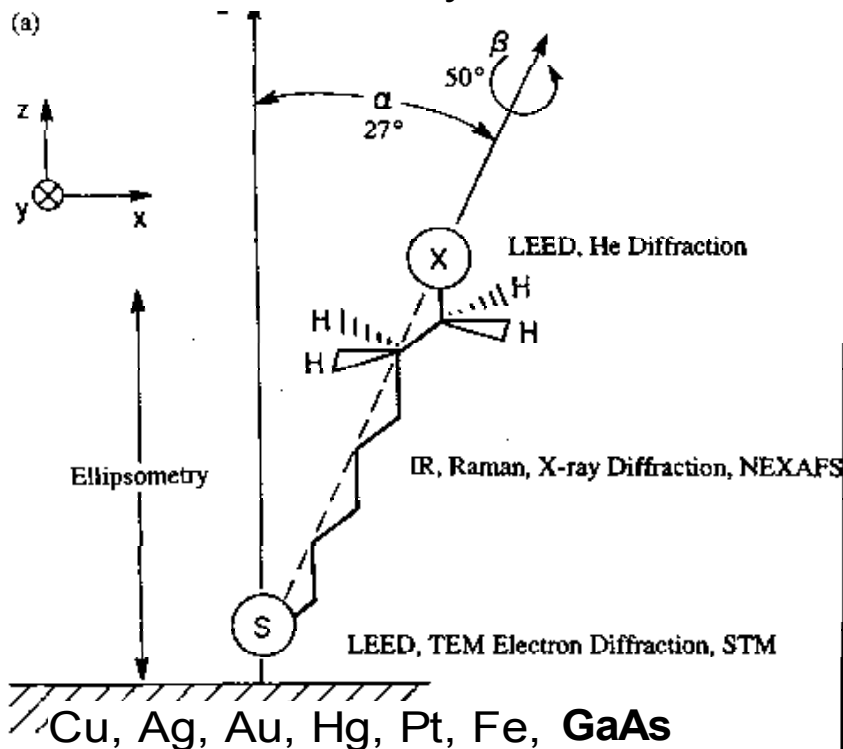


**Figure 7.** The UV/vis spectra (hexane) of dodecanethiolate-protected Au clusters: (a) ( $-78^\circ$ , 2X, sd),  $C = 3 \times 10^{-6}$  M, MW =  $3.4 \times 10^4$  amu; (b) ( $90^\circ$ , 2X, sd),  $C = 2 \times 10^{-6}$  M, MW =  $5.5 \times 10^4$  amu; (c) (RT, 1/3X, fd),  $C = 4 \times 10^{-7}$  M, MW =  $2.3 \times 10^5$  amu; (d) (RT, 1/4X, fd),  $C = 2 \times 10^{-7}$  M, MW =  $5.5 \times 10^5$  amu; (e) (RT, 1/12X, fd),  $C = 9 \times 10^{-8}$  M, MW =  $1.1 \times 10^6$  amu.

# 1c. analysis and application of alkanethiol SAMs

Dubois & Nuzzo Annual Rev. Phys. Chem., 1992, 43, 437-463

dense, ordered, crystalline, 5-30Å



2. vibrational spectroscopy  
**structure**

3. electrochemical methods  
**barrier properties**

4. surface plasmon  
resonance spectroscopy  
**optical thickness**

5. in-plane conductivity  
of Au films  
**extent of chemisorption**

6. electrochemical control  
of adsorption  
**new directions**

Corrosion inhibition

Tribology

Wetting and adhesion

Nanolithography

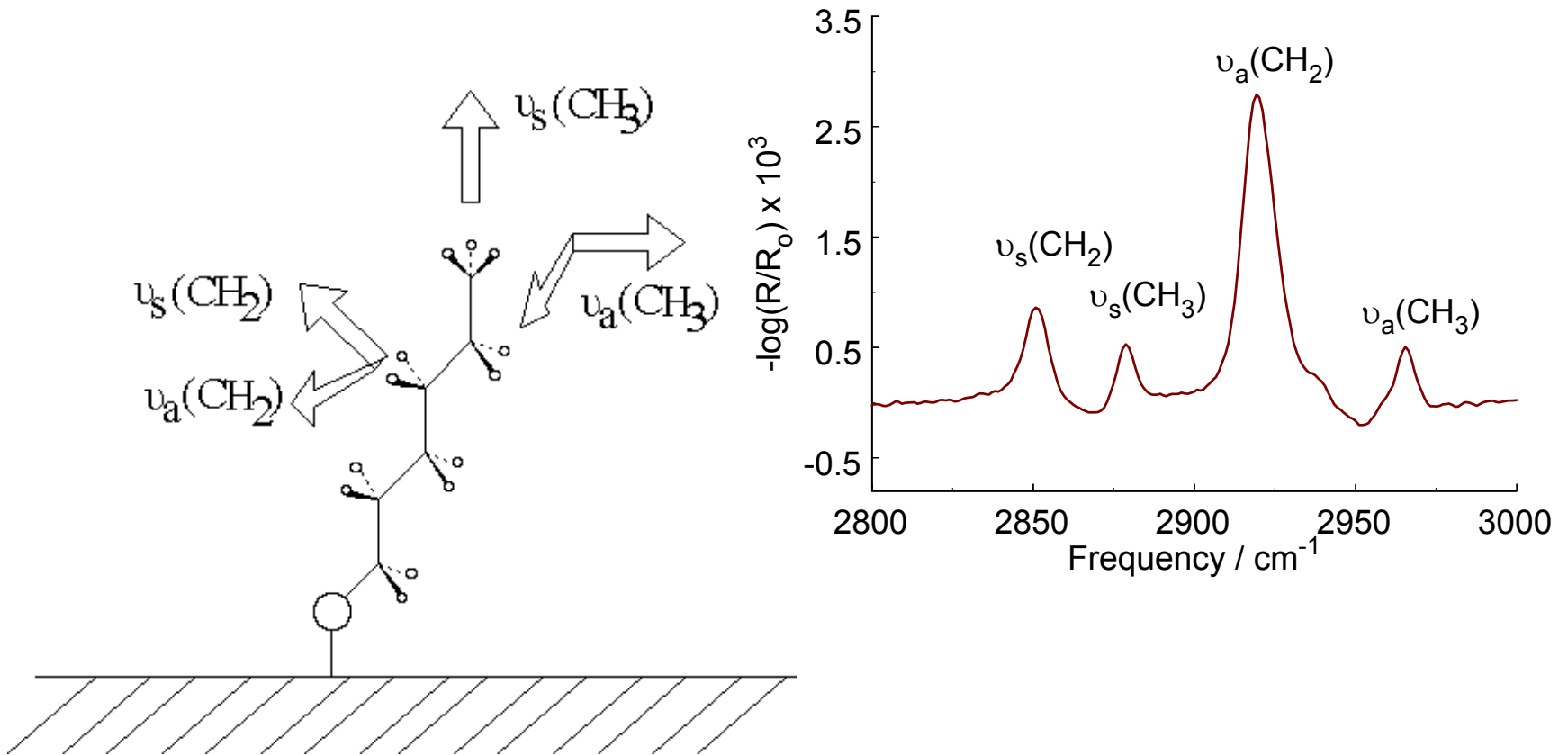
Electron transfer research

sensor / surface design:

Rubinstein et al.  
*Nature* 1988, 332,

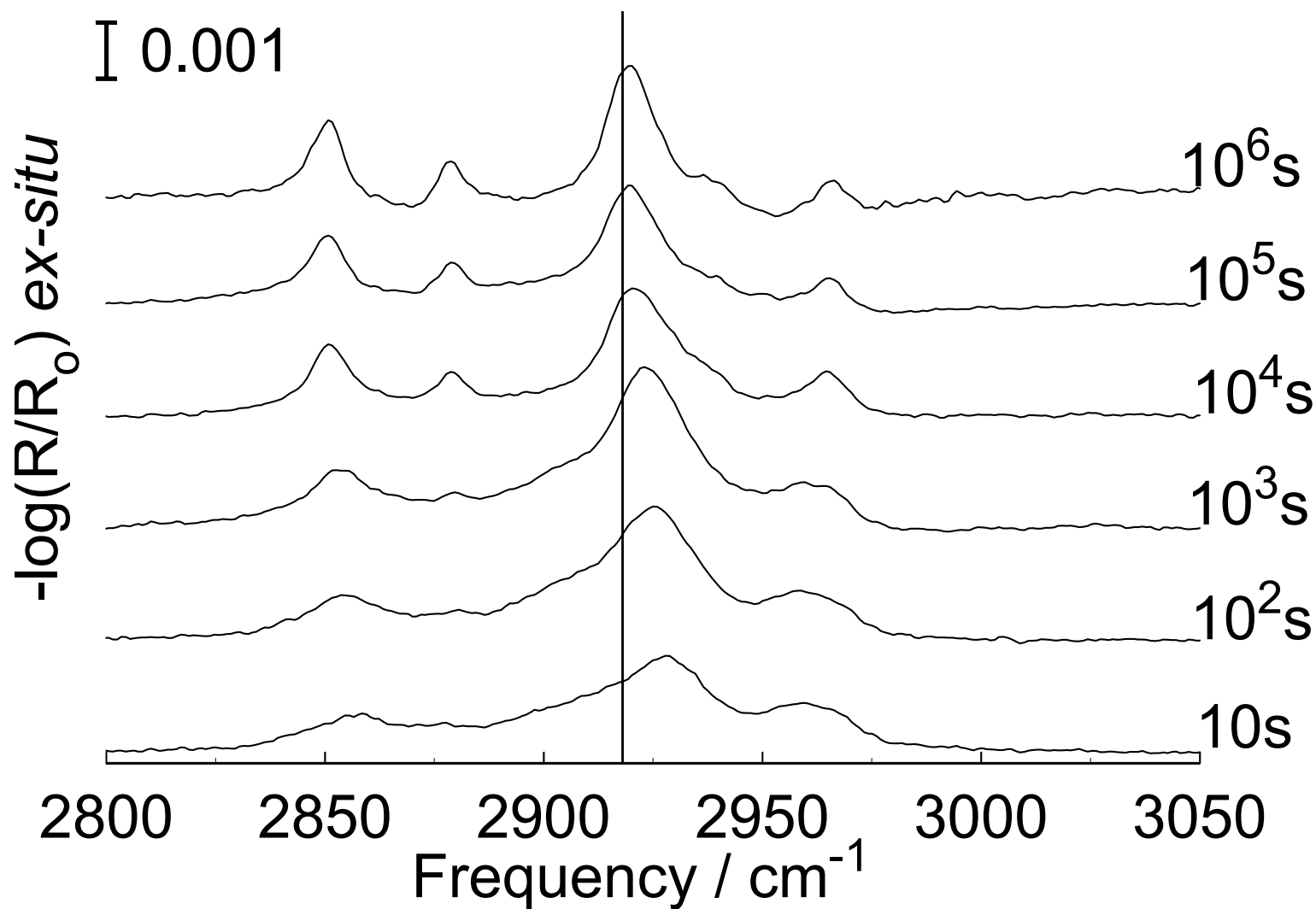
Majda et al. *J. Am. Chem. Soc.*  
1991, 113, 5654.

## 2a. C-H stretching modes by infrared reflection-absorption

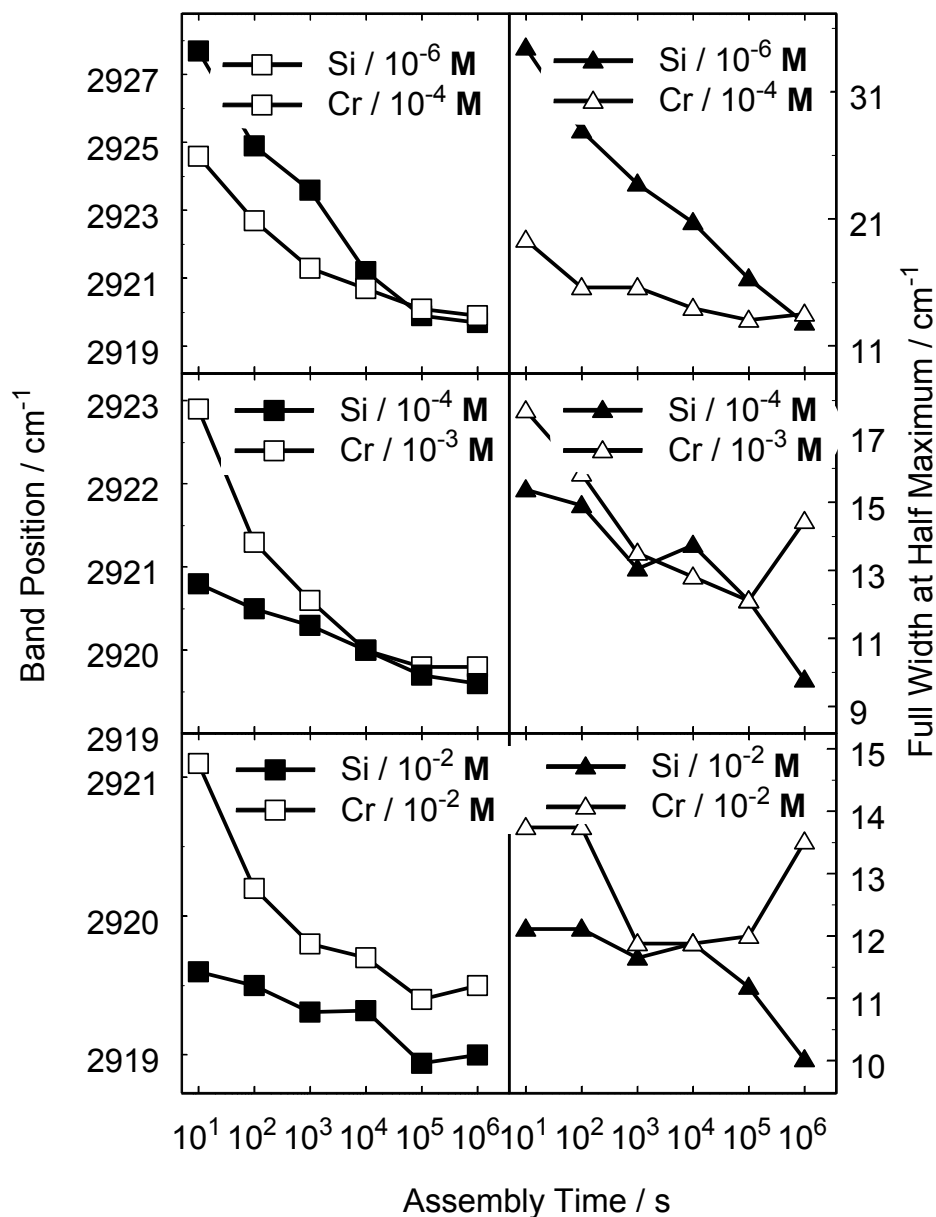


*2b. time evolution of C-H stretching bands*

Si[111]|Au(1500Å)| $10^{-6}$  M hexadecanethiol / ethanol



## 2c. $\nu_a(\text{CH}_2)$ band width and position



1. All shifts are bathochromic.
2. Higher [RSH] favors bigger, faster shifts.
3. Smoother, Si-H | Au favors bigger, faster shifts.
4. Changes can continue to  $10^5$  or  $10^6$  s.
5. Changes consistent with chain crystallization.

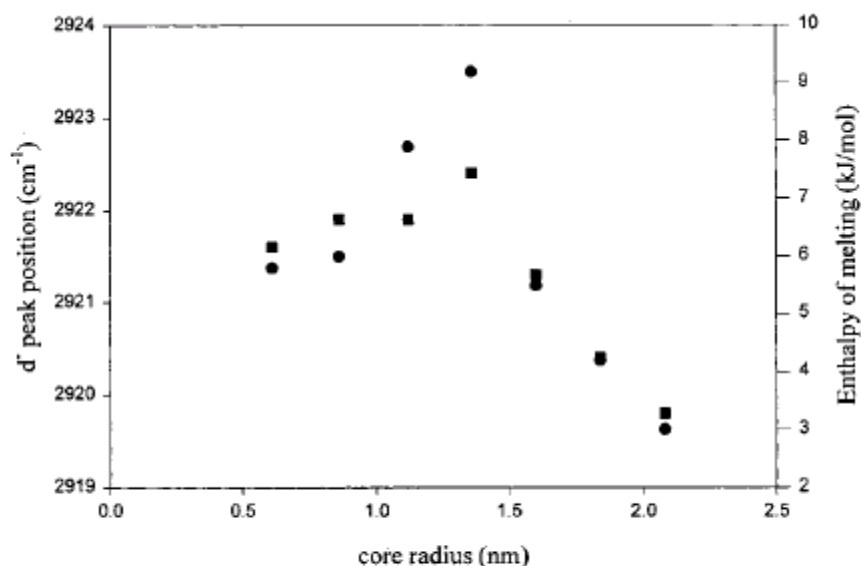


**Figure 8.** Plot of the  $d^*$  peak position (■), which tracks the amount of *gauche* defects in the ligand shell, and the enthalpy of melting (●) as a function of the radius of the dodecanethiolate-protected Au cluster cores.

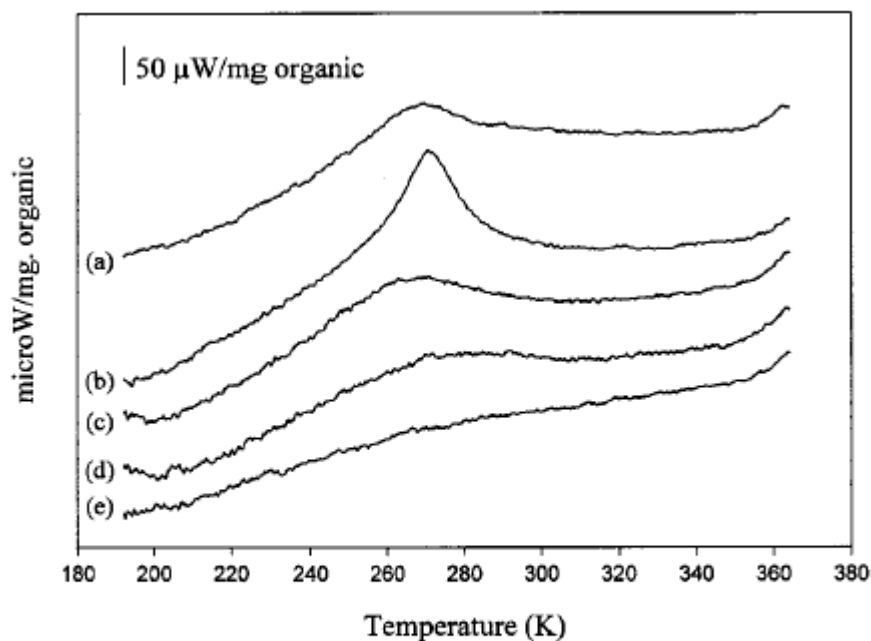


**Figure 9.** Differential scanning calorimetric traces (cooling curve) of solid-state samples of dodecanethiolate-protected Au cluster compounds: (a) ( $-78^\circ$ , 2X, sd); (b) ( $90^\circ$ , 2X, sd); (c) (RT, 1/3X, fd); (d) (RT, 1/4X, fd); (e) (RT, 1/6X, fd).

## Structural Evolution of Hexadecanethiol Monolayers on Gold during Assembly: Substrate and Concentration Dependence of Monolayer Structure and Crystallinity

Roger H. Terrill, Troy A. Tanzer, and Paul W. Bohn\*

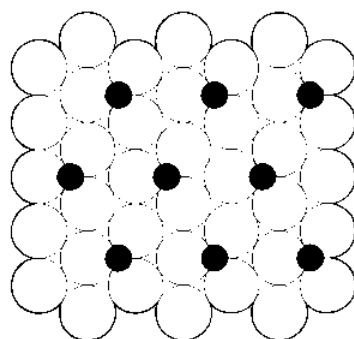


**Figure 1.** Representation of the  $\sqrt{3} \times \sqrt{3}$  (R30°) overlay structure for thiol S-headgroups (filled circles) binding to a gold surface (open circles).

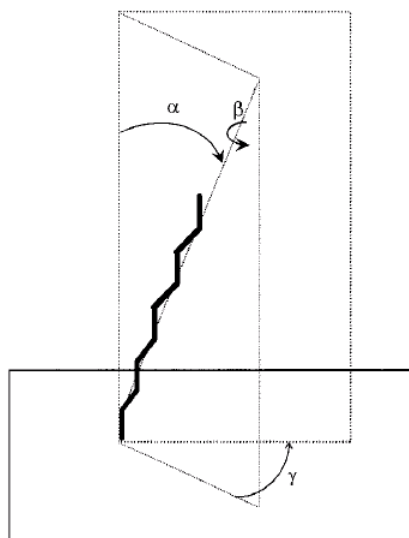


**Figure 2.** Alkanethiol chain configuration showing chain cant angle ( $\alpha$ ), chain twist angle ( $\beta$ ), and azimuthal angle ( $\gamma$ ) with respect to gold surface crystal axis.

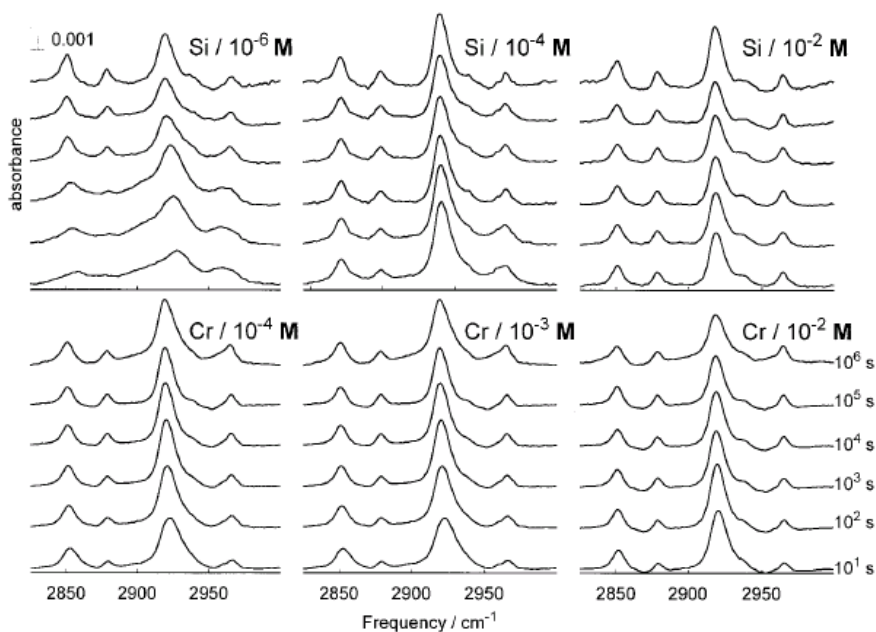


**Figure 4.** FTIR-ERS spectra of assembling HDT films. "Si" denotes HF-etched Si[111] anchored Au. "Cr" indicates a Cr-primed glass substrate for the Au film. HDT assembly solution concentration is indicated by numbers at upper right of spectral ensembles. Assembly times vary from  $10^1$  to  $10^6$  s on all graphs from bottom to top.

**Table 1. Assignments and Peak Frequencies of Major CH Stretching Bands**

		band frequencies/cm <sup>-1</sup>			
		CH <sub>3</sub> (a)	CH <sub>2</sub> (a)	CH <sub>3</sub> (s)	CH <sub>2</sub> (s)
	liquid thiol <sup>46</sup>		2924		2855
	solid thiol <sup>46</sup>		2918		2851
	shift <sup>a</sup>		-6		-4
0.1 mM	glass Cr Au HDT 10 s	2966.0	2924.8	2879.5	2854.1
	glass Cr Au HDT 10 <sup>6</sup> s	2965.3	2920.0	2878.8	2851.1
	shift <sup>b</sup>	-0.7	-5.2	-0.7	-3.0
0.1 mM	Si[111] Au HDT 10 s	2964.6	2920.7	2878.8	2851.5
	Si[111] Au HDT 10 <sup>6</sup> s	2964.9	2919.7	2878.7	2850.7
	shift <sup>b</sup>	+0.3	-1.0	-0.1	-0.8

<sup>a</sup> Shift defined as the difference in peak positions of the solid and liquid thiols. <sup>b</sup> Shift defined as the difference in peak positions of the 10<sup>6</sup> and 10 s assembly time films.

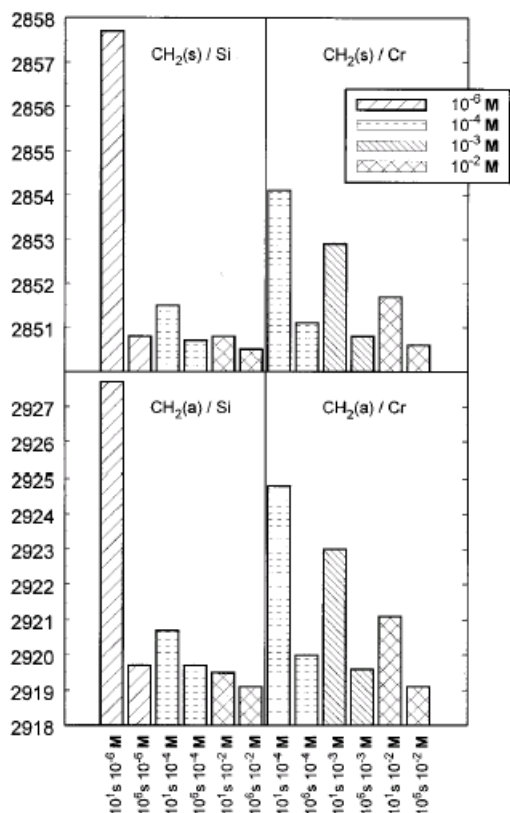


**Figure 5.** A comparison of the CH<sub>2</sub> band positions at 10 and 10<sup>6</sup> s for HDT films on both Si- and Cr-anchored Au and using a common scale. Note that for the Si[111]-anchored Au, the assembly was from 10<sup>-6</sup>, 10<sup>-4</sup>, and 10<sup>-2</sup> M HDT but for the (glass|Cr anchor) assembly was from 10<sup>-4</sup>, 10<sup>-3</sup>, and 10<sup>-2</sup> M HDT. Concentration and assembly time increase going from left to right along the chart.

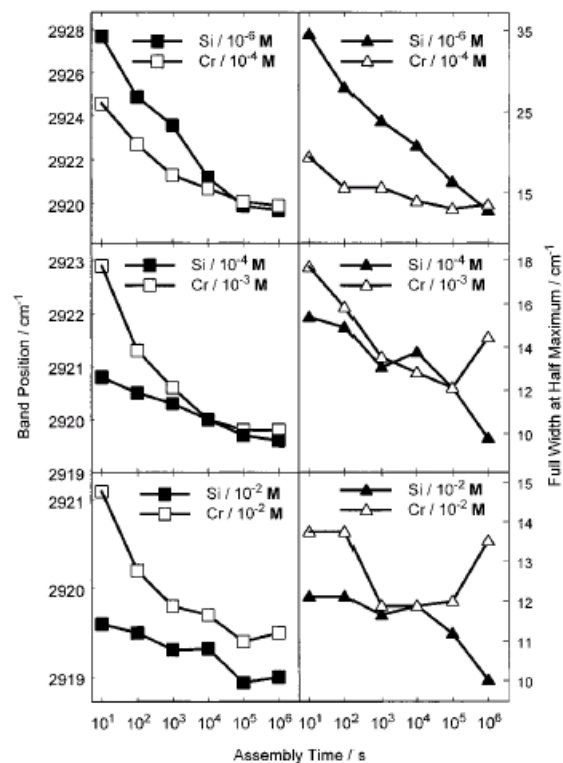


**Figure 6.** A comparison of peak frequency (squares, left side) and peak full-width at half-maximum (fwhm, triangles, right side) of  $\nu_a(\text{CH}_2)$  for all times and concentrations on both Si-anchored Au films (filled symbols) and Cr-anchored films (open symbols). Note that top panels compare assembly onto Si-anchored Au from 10<sup>-6</sup> M HDT to assembly onto glass|Cr-anchored Au from 10<sup>-4</sup> M HDT, and middle panels similarly compare assembly onto Si-anchored Au from 10<sup>-4</sup> M HDT to assembly onto glass|Cr-anchored Au from 10<sup>-3</sup> M HDT.